Study of selective amorphous silicon etching to silicon nitride using a pin-to-plate dielectric barrier discharge in atmospheric pressure

Se-Jin Kyung,[a] Jae-Beom Park, June-Hee Lee, Jong-Tae Lim, and Geun-Young Yeom[b]
Department of Advanced Materials Science and Engineering, Sungkyunkwan University, Jangan-Gu, Chunchun-Dong 300, Suwon 440-746, South Korea

(Received 8 June 2007; accepted 12 August 2007; published online 30 August 2007)

Remote-type atmospheric pressure plasmas were generated using a modified dielectric barrier discharge with the powered electrode consisting of multipins instead of a conventional blank planar plate. For the N_2/NF_3 gas mixture, a high etch rate of a:Si close to 115 nm/s was obtained by adding 300 SCCM (SCCM denotes cubic centimeter per minute at STP) of NF_3 to N_2 [50 SLM (standard liters per minute)] at an ac rms voltage of 8.5 kV (2.5 kW, 30 kHz). However, the selectivity of a:Si to Si_3N_4 was as low as 1.3. A selectivity of a:Si/$Si_3N_4 > 5.0$ could be obtained while maintaining an etch rate of a:Si at 110 nm/s by adding 250 SCCM CF_4 to the N_2 (50 SLM)/NF_3 (300 SCCM) mixture through the formation of a C–F polymer layer preferentially on the Si_3N_4 surface. © *2007 American Institute of Physics*. [DOI: 10.1063/1.2779096]

In flat panel display (FPD) processing such as the etching of a:Si, SiO_2, and Si_3N_4 films, in-line processing that does not require a vacuum chamber is necessary for satisfying the low-cost, high throughput processes for the next generation of display processing.[1,2] One of the candidates for in-line processing is atmospheric pressure plasma processing. Among the many atmospheric pressure plasmas, plasmas that can generate a uniform glow discharge, such as dielectric barrier discharge (DBD),[3] capillary electrode discharge,[4] microwave discharge,[5] plasma jet,[6] and hollow cathode discharge,[7] have been investigated.

Among the various atmospheric pressure plasmas, DBD, which has dielectric plates on one or both of the parallel electrodes, is generally applied to FPD processing because it is easily expandable to a larger size and a glow discharge type with uniform plasma over the entire substrate area. However, conventional DBD has a high breakdown voltage and a low plasma density due to the high recombination rate at atmospheric pressure. Therefore, it is difficult to apply conventional DBD to the high speed etching processing such as the etching of a:Si, SiO_2, Si_3N_4, etc.[8]

In this study, a modified DBD consisting of a multipin powered electrode instead of a planar powered electrode was used to generate high density plasma at a low breakdown voltage.[9] In particular, a remote plasma-type configuration was used in an attempt to prevent damage to the surface of the samples during atmospheric pressure plasma processing. The characteristics of the remote-type pin-to-plate DBD such as the electrical characteristics, plasma characteristics, etch rate, and etch selectivity of the a:Si and Si_3N_4 in $N_2/NF_3/CF_4$ gas mixtures were investigated.

Figure 1 shows the remote-type pin-to-plate DBD used for etching a:Si and Si_3N_4. The discharge source consisted of two parallel electrodes installed vertically above the sample surface, which are a multipin powered electrodes and a blank ground electrode. These electrodes were coated with alumina (Al_2O_3). ac power (30 kHz) of 8.5 kV (rms voltage) was applied to the powered multipin electrode to generate the atmospheric pressure plasmas.

As the discharge gas, NF_3 [(0–600 SCCM (SCCM denotes cubic centimeter per minute at STP)] and CF_4 (0–300 SCCM) added to 50 SLM (standard liters per minute) of N_2 were used to etch the a:Si and Si_3N_4. CF_4 gas was used to improve the etch selectivity between a:Si and Si_3N_4. a:Si deposited on a Si_3N_4/glass substrate, Si_3N_4 deposited on a glass substrate and patterned using a photoresist were used as samples. The voltage and current of the atmospheric pressure plasmas were measured for the consumed power calculation using a high voltage probe (Tektronix P6015A) and a current probe (Pearson electronics 6600), respectively. The species in the plasma were measured using optical emission spectroscopy (OES) (SC Tech. PCM-420). X-ray photoelectron spectroscopy (XPS) (Thermo VG, SIGMA PROBE) was also used to examine the etch products

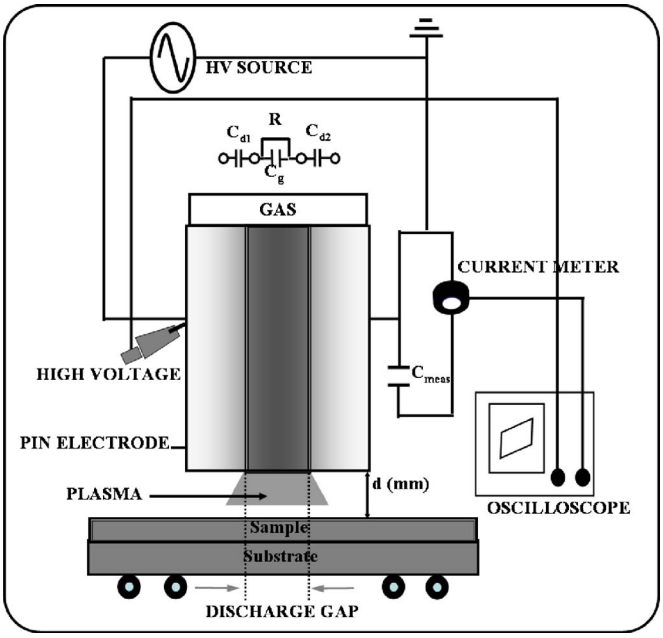

FIG. 1. (Color online) (a) Schematic diagram of the atmospheric pressure plasma system used in this study (pin-to-plate DBD).

[a]Electronic mail: magnatic@skku.edu
[b]Author to whom correspondence should be addressed; electronic mail: gyyeom@skku.edu

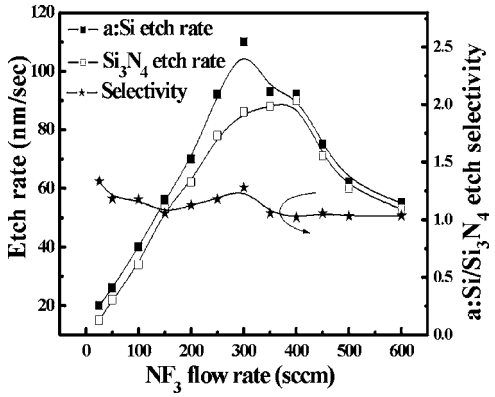

FIG. 2. Effect of the NF_3 flow rate in the N_2 (50 SLM)/NF_3 (25–600 SCCM) gas mixture on the etch rates of a:Si and Si_3N_4 and the etch selectivity of a:Si to Si_3N_4.

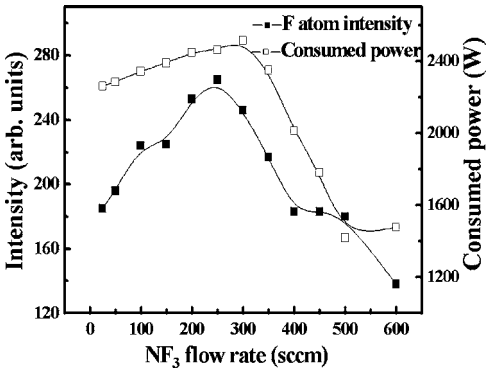

FIG. 3. Effect of the NF_3 flow rate in the N_2 (50 SLM)/NF_3 (25–600 SCCM) gas mixture on the power consumption and the relative optical emission intensity of F (704 nm) measured by OES.

remaining on the etched a:Si and Si_3N_4 surfaces. A Mg Kα source was used to provide a monochromatic x ray at 1253.6 eV. The C 1s photoemission at 284.5 eV was used as the reference binding energy.

Figure 2 shows the etch rate of the a:Si and Si_3N_4 and the etch selectivity of a:Si to Si_3N_4 measured as a function of the NF_3 flow rate added to 50 SLM of N_2. As shown in the figure, the addition of NF_3 at flow rates ranging from 25 to 300 SCCM increased the etch rate of a:Si from approximately 20 to 115 nm/s. However, further increases in the NF_3 flow rate to 600 SCCM decreased the etch rate of a:Si significantly. The etch rate of Si_3N_4 showed a similar trend as that of a:Si but the etch rate of Si_3N_4 was slightly lower than that of a:Si, showing a maximum etch rate of 85 nm/s at 300 SCCM of NF_3. Therefore, the etch selectivity of a:Si to Si_3N_4 was low ranging from 1.0 to 1.3.

Optical emission spectra of the plasmas generated by the pin-to-plate DBD were measured as a function of the NF_3 flow rate. Figure 3 shows the change in the F atomic emission peak observed at 704 nm.[10] As shown in the figure, the addition of 300 SCCM NF_3 showed a maximum F emission intensity and a further increase in NF_3 drastically decreased the optical emission intensity. Figure 3 also shows the power consumption in the reactor measured as a function of the NF_3 flow rate at an applied voltage of 8.5 kV (30 kHz). The consumed power was calculated by the Q-V Lissajou curve showing the charge accumulated in the discharge system as a function of instant ac voltage to the powered electrode. As shown in the figure, the power consumption in the reactor at a given applied ac voltage to the powered electrode increased with increasing NF_3 up to 300 SCCM, which is similar to the F atomic emission intensity. The increase in power consumption with increasing NF_3 up to 300 SCCM is related to a decrease in the breakdown voltage and an increase in the plasma-on time estimated from the Q-V Lissajou plot by the addition of NF_3. However, the decrease in the power consumption with increasing NF_3 flow rate $>$300 SCCM is believed to be related to the transition of the plasma mode from a uniform glow-type discharge to a filamentary-type discharge, as can be directly observed from the plasma. In fact, it could not be identified whether the glow-type discharge does not contain any microscopic filamentary discharge even though the discharge appeared to be a uniform glow discharge; however, the plasma generated with a NF_3 flow rate higher than 300 SCCM showed a clear filamentary discharge between the electrodes and the amount of filamentary discharge increased with the increase of NF_3 flow rate. The increase in the F atomic emission intensity observed with increasing NF_3 flow rate up to 300 SCCM in Fig. 3 is not only related to the increase in the electron density in the plasma, as can be estimated by the increase in power consumption at a constant voltage, but also to the increase in F atomic density by the increased dissociation of NF_3 molecules. This is due to the fact that the increased F atomic intensity (from 185 to 265) is higher than the increased power consumption (from 2260 to 2500 W) with increasing NF_3 from 25 to 300 SCCM. Further increases in the NF_3 flow rate decreased the F atomic density due to the decrease in the dissociation rate by forming an inefficient filamentary discharge. The change in a:Si and Si_3N_4 observed as a function of the NF_3 flow rate in Fig. 2 is related to the change in the F atomic density in the plasma because both a:Si and Si_3N_4 are easily etched by F atoms.

In order to improve the etch selectivity, CF_4 was added to the optimized condition of NF_3 shown in Fig. 2. Figure 4(a) shows the etch rate of a:Si and Si_3N_4 and the etch selectivity of a:Si to Si_3N_4 measured as a function of the CF_4 flow rate added to N_2 (50 SLM)/NF_3 (300 SCCM). As shown in the figure, the addition and increase in CF_4 to N_2 (50 SLM)/NF_3 (300 SCCM) did not produce a significant change in the a:Si etch rate, while the etch rate of Si_3N_4 decreased almost linearly with increasing CF_4 flow rate. Therefore, by increasing the CF_4 flow rate from 0 to 250 SCCM, the etch selectivity of a:Si to Si_3N_4 increased from 1.3 to 5.1. In order to understand the mechanism of the change in the etch selectivity, the etched surfaces of a:Si and Si_3N_4 were examined by XPS.

Figure 4(b) shows the XPS data of C 1s measured on the surfaces of the a:Si and Si_3N_4 after etching with N_2 (50 SLM)/NF_3 (300 SCCM) and N_2 (50 SLM)/NF_3 (300 SCCM)/CF_4 (250 SCCM). As shown in the figure, the surfaces of the a:Si(I) and Si_3N_4(II) after etching with N_2 (50 SLM)/NF_3 (300 SCCM) showed a similar binding peak near 284.5 eV, which was assigned to C–C bonding, as well as small binding peaks near 287.0 eV, which were assigned to C–F bonding, and near 289.5 eV from C–F_2 bonding. Therefore, no significant C–F polymer layer or a very sparse C–F polymer layer was formed on these etched surfaces. In addition, the lack of a significant change in the C 1s binding states could be observed for the surface of a:Si(III) after etching with N_2 (50 SLM)/NF_3 (300 SCCM)/CF_4

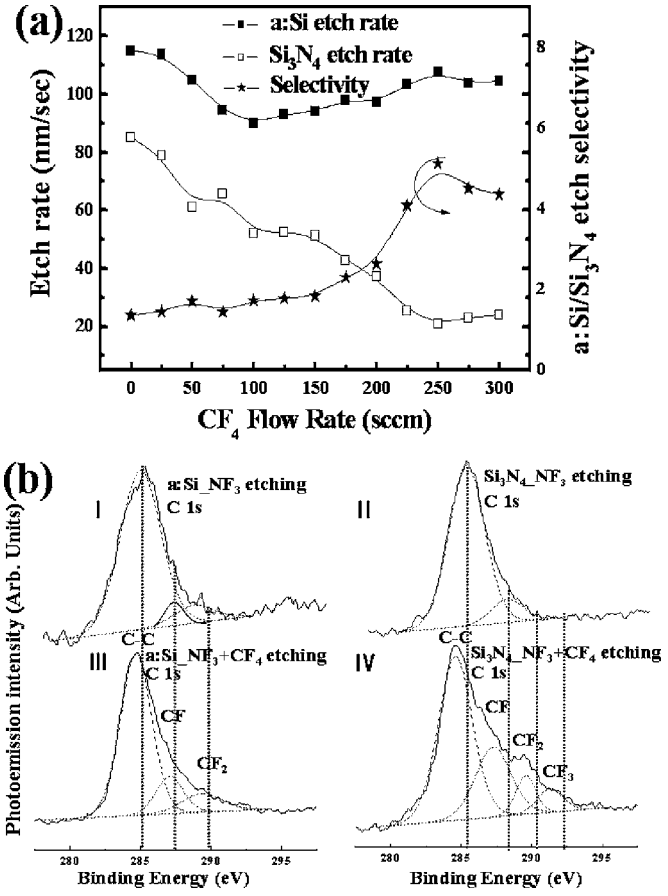

FIG. 4. (a) Effect of the CF_4 flow rate in the N_2 (50 SLM)/NF_3 (300 SCCM)/CF_4 (0–300 SCCM) gas mixture on the etch rates of a:Si and Si_3N_4 and the etch selectivity of a:Si to. (b) (I and II) C 1s XPS spectra of the a:Si and Si_3N_4 after the etching with N_2 (50 SLM)/NF_3 (300 SCCM). (III and IV) C 1s XPS spectra of the a:Si and Si_3N_4 after etching with N_2 (50 SLM)/NF_3 (300 SCCM)/CF_4 (250 SCCM).

(250 SCCM). In the case of the Si_3N_4(IV) surface after the etching with N_2 (50 SLM)/NF_3 (300 SCCM)/CF_4 (250 SCCM), the significant intensities of the C 1s binding peaks related to CF (287.2 eV), CF_2 (289.5 eV), and CF_3 (291.2 eV) could be observed indicating the formation of a thicker or denser C–F polymer layer on the etched Si_3N_4 surface. Therefore, the decrease in the Si_3N_4 etch rate with increasing CF_4 flow rate is believed to be related to the formation of a thicker or denser C–F polymer layer on the Si_3N_4 surface, which prevents the diffusion of F to the surface of Si_3N_4 for etching. In general, the addition of CF_4 tends to form a C–F polymer preferentially on a silicon surface than the Si_3N_4 surface because in the case of Si_3N_4, carbon can be removed from the Si_3N_4 surface by forming volatile CN, while carbon on the silicon surface can be removed only by additional F atoms.

However, as shown in Fig. 4(b) a sparse or no significant C–F polymer layer was formed on the etched a:Si surface compared with the etched Si_3N_4 surface. The sparse or no significant C–F polymer layer on the etched a:Si surface is believed to be related to the lower binding energy between Si–Si in the amorphous states. In the case of a:Si, compared with crystalline silicon, fewer F atoms might be required for vaporization and etching. (In fact, for a same atmospheric pressure plasma etch condition, the etch rate of a:Si is about 1.7 times faster than that of the crystalline silicon.) Therefore, more incoming F atoms might be available for removing carbon atoms on the a:Si surface, which causes a sparse C–F polymer layer on the surface. Therefore, due to the differences in the C–F polymer formation on the a:Si and Si_3N_4, an etch selectivity of a:Si to $Si_3N_4 > 5.0$ could be obtained by adding 250 SCCM of CF_4 to N_2 (50 SLM)/NF_3 (300 SCCM) without altering the etch rate of a:Si significantly.

In this study, to obtain higher plasma density compared to the conventional DBD, a modified pin-to-plate DBD was used, and its discharge characteristics as well as the etch characteristic of a:Si and Si_3N_4 were investigated. With N_2/NF_3, the etch selectivity ranged from 1.0 to 1.3. The etch selectivity of a:Si to Si_3N_4 was increased by adding CF_4 to N_2/NF_3 without significantly decreasing the etch rate of a:Si. The increase in the etch selectivity was related to the formation of a C–F polymer preferentially on the etched Si_3N_4 surface. A maximum etch rate of a:Si of 110 nm/s and an etch selectivity of a:Si/$Si_3N_4 > 5$ could be obtained with a gas mixture of 250 SCCM CF_4 in N_2 (50 SLM)/NF_3 (300 SCCM) and at 30 kHz ac rms voltage of 8.5 kV.

This work was supported by the National Program for Tera-Level Nanodevices of the Korea Ministry of Science and Technology as a 21st Century Frontier Program.

[1]K. N. Kim, J. H. Lim, and G. Y. Yeom, Appl. Phys. Lett. **89**, 251501 (2006).
[2]M. Iwasaki, M. Ito, T. Uehara, M. Nakamura, and M. Hori, J. Appl. Phys. **100**, 093304 (2006).
[3]Q. Y. Nie, C. S. Ren, D. Z. Wang, S. Z. Li, J. L. Zhang, and M. G. Kong, Appl. Phys. Lett. **90**, 221504 (2007).
[4]S. J. Kyung, Y. H. Lee, C. W. Kim, J. H. Lee, and G. Y. Yeom, Carbon **44**, 1530 (2006).
[5]J. T. Krile, A. A. Neuber, H. G. Krompholz, and T. L. Gibson, Appl. Phys. Lett. **89**, 201501 (2006).
[6]Y. Sakurai, T. Kobayashi, Y. Hasegawa, and H. Shirai, Jpn. J. Appl. Phys., Part 1 **44**, 749 (2005).
[7]T. I. Lee, K. W. Park, H. K. Baik, and S. M. Lee, Appl. Phys. Lett. **87**, 261502 (2005).
[8]K. Yamakawa, M. Hori, T. Goto, S. Den, T. Katagiri, and H. Kano, Appl. Phys. Lett. **85**, 549 (2004).
[9]Y. H. Lee and G. Y. Yeom, Jpn. J. Appl. Phys., Part 1 **44**, 1076 (2005).
[10]K. Yamakawa, M. Hori, T. Goto, S. Den, T. Katagiri, and H. Kano, J. Appl. Phys. **98**, 013301 (2005).